Potential Vorticity Asymmetries and Tropical Cyclone Motion

LLOYD J. SHAPIRO

Department of Atmospheric Science, Colorado State University, Fort Collins, Colorado

JAMES L. FRANKLIN

Hurricane Research Division, NOAA/AOML, Miami, Florida

(Manuscript received 22 January 1998, in final form 19 March 1998)

ABSTRACT

A set of nine synoptic-flow cases, incorporating Omega dropwindsonde observations for six tropical storms and hurricanes, is used to deduce the three-dimensional distribution of potential vorticity (PV) that contributed to the deep-layer mean (DLM) wind that steered the cyclones. A piecewise inversion technique, the same as that previously applied by Shapiro to Hurricane Gloria of 1985, is used to derive the DLM wind induced by pieces of anomalous PV restricted to cylinders of different radii centered on each cyclone. The cylinder of PV that induces a DLM wind that best matches the observed DLM wind near the center of each cyclone is evaluated.

It is found that the results can be loosely placed into two categories describing the spatial scale of the PV anomalies that influenced the cyclone's motion. Four of the cases, including Hurricane Gloria, had ''local'' control, with a good match (to within ~40%) between the observed DLM wind near the cyclone center and the DLM wind attributable to a cylinder of PV with a given radius $\leq$1500 km. Further decomposition of the PV anomaly into upper (400 mb and above) and lower levels (500 mb and below) indicates the dominance of upper-level features in steering two of the cyclones (Hurricanes Gloria of 1985 and Andrew of 1992), while Hurricane Debby of 1982 was steered by more barotropic features. These results supplement those found in other studies.

Five of the cases, by contrast, had ''large-scale'' control, with no cylinder of radius $\leq$2000 km having a good match between the induced and observed DLM wind. Hurricanes Emily of 1987 and 1993 fell into this category, as did Hurricane Josephine of 1984. Implications of the results for guiding in situ wind measurements to improve hurricane track forecasts are discussed.

1. Introduction

a. Background

It has been clearly established that the deep-layer mean (DLM) flow near a tropical cyclone is strongly related to its motion averaged over a 12-h period (Franklin et al. 1996; also see review in section 2a of Wu and Emanuel 1995a). Potential vorticity (PV) inversion is a powerful tool that can be applied to understanding the factors that contribute to this motion. Given an appropriate balance condition, boundary conditions, and background state, a PV anomaly can be inverted to uniquely derive the complete three-dimensional wind and temperature distribution associated with the PV. Previous studies (Wu and Emanuel 1995a,b; Wu and Kurihara 1996) have used a piecewise inversion technique (Davis and Emanuel 1991) to evaluate the influence of upper- and lower-level PV anomalies on the motion of several hurricanes. These studies emphasized the contribution of upper-level anomalies on the flow that steered the hurricanes.

Recently a new piecewise inversion technique has been developed and applied to Hurricane Gloria of 1985 (Shapiro 1996, hereafter S96). For this hurricane Omega dropwindsonde (ODW) observations in the storm environment were supplemented by Doppler winds near its center (Franklin et al. 1993; Shapiro and Franklin 1995). Motivated by the weak asymmetries in the core of Gloria (Shapiro and Montgomery 1993), the piecewise inversion technique, described explicitly in the appendix of S96, decomposes the horizontal wind into symmetric (vortex) and asymmetric (environmental) components. Since the large-scale winds that determine a storm's average motion are nearly nondivergent, the nonlinear balance equation can be used to derive the geopotential from the streamfunction. The basic-state geopotential is derived from the symmetric basic-state streamfunction, and the basic-state potential vorticity is derived from these quantities. Anomalies are then defined as deviations between the total fields and the corresponding basic states.

Corresponding author address: Dr. Lloyd J. Shapiro, Meso and Micrometeorology, Meteorological Institute, University of Munich, Theresienstrasse 37, 80333 Munich, Germany.

The PV and balance equations involve nonlinear products between anomalies. In practice, however, the nonlinear terms in the case of Hurricane Gloria were found to be small. Thus, a *linear* decomposition could be made that associated a given piece of PV with a given height and wind distribution.[1] The ad hoc nature of the piecewise decomposition required by Davis and Emanuel (1991)[2] and Wu and Emanuel (1995a,b) was thereby avoided. Moreover, since the hurricane vortex is identified with the symmetric basic state, removal of the hurricane vortex and use of a climatological basic state were avoided as well. On the upper and lower boundaries potential temperature and corresponding vertical shear of the anomalies were specified. Homogeneous conditions are required on the lateral boundaries since the contribution of each piece of PV to the boundary winds is not known. The lateral boundaries were found, in fact, to have a very small effect on the results for Gloria.

In a set of benchmark analyses, S96 evaluated the wind anomalies attributable to pieces of anomalous PV restricted to cylinders of different radii centered on Gloria. It was found that the DLM wind that steered Gloria to the northwest was primarily attributable to PV anomalies confined within a cylinder of radius 1000 km and levels 500 mb and above, with more than five-sixths of the hurricane's motion explained. The results implied that in order to improve prediction of short-term changes in the environmental flow field that steered Gloria, measurements of upper-level winds and heights are required at least out to 1000 km.

b. Synoptic-flow cases

A larger sample of cases is required to evaluate how representative the result for Gloria is. In the present paper the results for Gloria are extended by performing piecewise inversions for other tropical cyclones, in order to deduce the three-dimensional distribution of PV that contributed to the DLM steering flow. In 1982, the National Oceanic and Atmospheric Administration's (NOAA) Hurricane Research Division began a series of ''synoptic-flow'' experiments using ODWs released from one or both of the NOAA WP-3D research aircraft to improve the quantity and quality of observations in the environment of tropical cyclones. Franklin et al. (1996, hereafter FFKA) describe the analysis of the wind fields for 17 experiments conducted from 1982 to 1992. From this sample, nine synoptic-flow cases (including Hurricane Gloria, Hurricane Emily of 1993, and seven additional cases described in section 2 of FFKA) for six tropical storms and hurricanes were chosen for PV analysis (Table 1). The cases chosen were essentially those with the best data distributions; in particular, all but one case (D1) involved a two-aircraft experiment.

TABLE 1. Synoptic-flow experiments analyzed (except for Hurricane Emily of 1993, following Franklin et al. 1996). The time is the nominal (central) time of the experiment. Here ID is a label for each case used in subsequent tables and figures. The motion vector, a 12-h mean, is specified by direction toward (measured clockwise from north) and speed. Maximum winds and motion vectors are from the NHC best track data.

Storm name	ID	Date/time (UTC)	Max wind ($m\ s^{-1}$)	Motion ($^{\circ}/m\ s^{-1}$)
Debby	D1	15 Sep 1982/0000	34	033/6.4
Debby	D2	16 Sep 1982/0000	49	027/8.9
Josephine	J1	10 Oct 1984/0000	26	341/2.2
Josephine	J2	11 Oct 1984/0000	39	008/3.4
Josephine	J3	12 Oct 1984/0000	46	007/3.9
Gloria	G1	25 Sep 1985/0000	62	313/6.2
Emily	E2	25 Sep 1987/0000	23	040/14.1
Andrew	A1	23 Aug 1992/0000	46	266/6.5
Emily	E3	30 Aug 1993/0000	36	314/3.4

As with the Gloria benchmark analyses, the wind fields analyzed by FFKA for the synoptic-flow cases are based on the spectral application of the finite element representation, developed by Ooyama (1987). The multinested synoptic-flow analyses are derived on meshes with effective resolved scales ranging from about 160 km down to 70 km near the hurricane. All 10 mandatory levels from 1000 to 100 mb, excluding 925 mb, are analyzed. Although these analyses do not incorporate Doppler data in the vortex core and therefore do not have as complete a data coverage as for Gloria, they incorporate special enhanced high-density satellite datasets and commericial aircraft reports that supplement ODW winds at levels above 400 mb (see section 3 of FFKA). Eight of the nine cases are analyzed over a domain extending about 2000 km from the storm's center, while Emily of 1993 is analyzed over a domain extending to about 4000 km.

As one example, Fig. 1 displays the PV anomalies, q', based on the synoptic-flow analyses for Hurricane Gloria (G1) at 250 and 700 mb over a disk of radius 2000 km centered on the hurricane. The PV anomaly is defined by

$$q' = q - \hat{q},$$

where q is Ertel's PV and $\hat{q}$ is the basic-state PV derived from the symmetric basic-state streamfunction and corresponding balanced geopotential, as described in section 2 of S96. These PV anomalies are generally similar to those derived from the filtered benchmark analyses of Gloria (cf. Fig. 4 of S96), with positive values at 250 mb to the southwest of the hurricane in the region of an upper-level cold low over Cuba. The PV anomalies at 700 mb clearly show a northwest–southeast oriented dipole localized near the hurricane.

[1] An effectively linear piecewise inversion has been recently made by Möller and Jones (1998) in a tropical cyclone modeling context using the asymmetric balance formulation of Shapiro and Montgomery (1993).

[2] The utility of the ad hoc decomposition was evaluated more completely by Davis (1992).

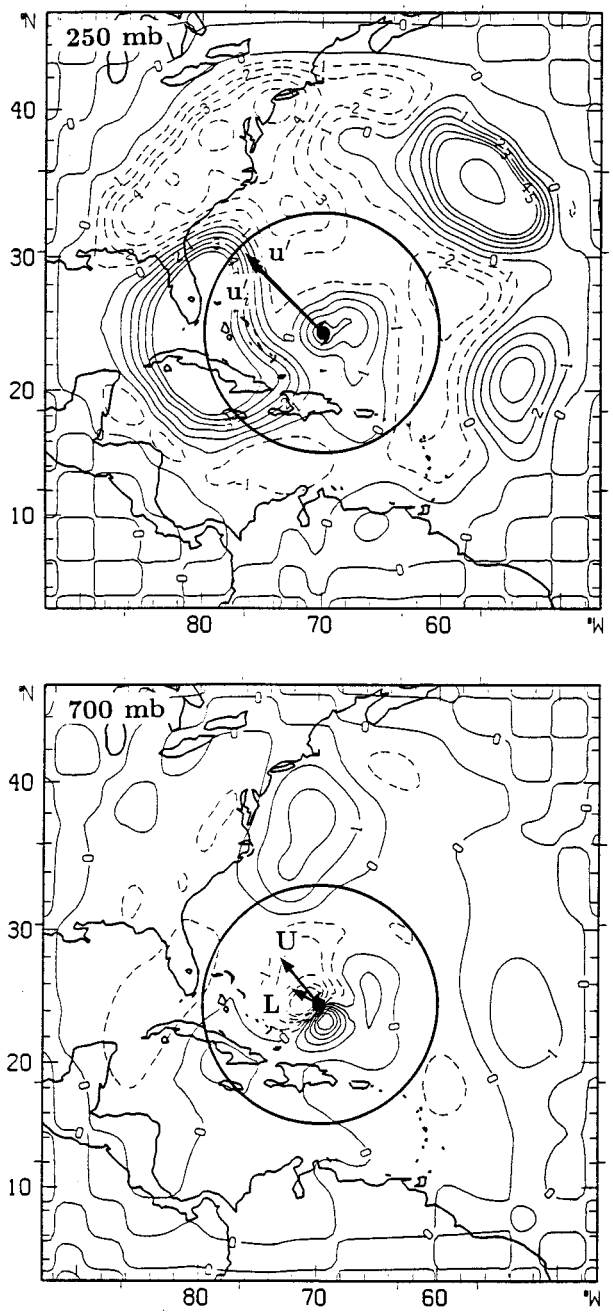

FIG. 1. Potential vorticity anomalies (q′) within 2000 km of the center of Hurricane Gloria (G1) at 250 (top panel) and 700 mb (bottom panel). Values outside 2000-km radius are set to 0. Contours are 0, ±1, ±2, ±3, ±4, ±5, 10, 15, 20 × 10^{-8} m^2 s^{-1} K kg^{-1}. Vectors in top panel indicate the observed DLM wind (**u**′) at radius r = 3° and the DLM wind ($\mathbf{u}_i'$) attributable to PV anomalies confined to a cylinder of radius 1000 km [shown (slightly distorted) by circles in both panels]. Vectors in bottom panel indicate contributions to $\mathbf{u}_i'$ from upper-level (400 mb and above) PV anomalies (**U**) and lower-level (500 mb and below) PV anomalies (**L**).

Using a linear piecewise inversion, S96 evaluated the DLM wind anomalies attributable to cylinders of anomalous PV centered on Hurricane Gloria, extending throughout the depth of the domain, with radii between 750 and 1500 km. It was found that the minimum difference between the deduced DLM wind at the center of the hurricane ($\mathbf{u}_i'$) and the hurricane's observed motion (**c**) was for a cylinder of radius 1000 km, with a vector difference $|\mathbf{u}_i' - \mathbf{c}| = 1.4$ m s^{-1}. This vector difference was much less than Gloria's 6.2 m s^{-1} translation speed. Cylinders with radii of 1250 and 1500 km were associated with DLM winds that were a poorer approximation to the hurricane's motion. The total analyzed DLM wind at the center of the hurricane (**u**′) differed from **c** by only 0.2 m s^{-1}; since the PV anomalies confined within a cylinder of sufficiently large radius would yield the analyzed DLM wind at the center, contributions to the DLM steering flow from PV anomalies outside of 1000-km radius must effectively cancel. Thus, the evolution of the DLM wind that steered Gloria was determined primarily by PV features within 1000 km of its center. In section 2 the results of the Gloria benchmark analyses are reevaluated from the synoptic-flow analyses and are extended to the other eight cases.

2. Results

As a preliminary to the piecewise inversions, the relationship between the motion of each of the nine tropical cyclones and its surrounding DLM flow is evaluated. FFKA found that tropical cyclone motion was consistent with barotropic steering of the vortex by the surrounding flow within 3° latitude (333 km) of the cyclone center. At this radius, the surrounding DLM flow explained over 90% of the variance in vortex motion for the 16 synoptic-flow cases analyzed. Due to analysis uncertainties, FFKA did not present any results for radii less than 3° from the cyclones' center. For our present analysis the agreement between the vortex motion (**c**) and the DLM wind (**u**′) was evaluated both at the center of each cyclone and at 3° radius. While the agreement was predominantly better at 3° radius, in two cases (A1, D2) the magnitude of the vector difference between the two quantities, $|\mathbf{u}' - \mathbf{c}|$, was smaller at the center (Table 2). The average difference for the nine cases at the radius of better agreement was 1.2 m s^{-1}, much greater than the 0.2 m s^{-1} difference found at the vortex center for the Hurricane Gloria benchmark analysis (S96). In order to fairly evaluate the degree to which the DLM wind derived from the piecewise inversion is related to the cyclones' motion, the DLM wind at the radius of better agreement (see Table 2) will be used as the basis of comparison.

For each of the nine synoptic-flow cases, the piecewise inversion was performed for PV anomalies confined to cylinders extending through the depth of the analysis (with boundary conditions applied at 100 and 1000 mb) with radii from 500 to 2000 km. In the case

TABLE 2. Magnitude of the vector difference, $|\mathbf{u}' - \mathbf{c}|$, between DLM wind ($\mathbf{u}'$) and motion of storm ($\mathbf{c}$) for each synoptic-flow experiment (ID) analyzed. The DLM wind is evaluated at the radius ($r = 0°$ or 3°) where the vector difference is smaller. The DLM wind is calculated for the layer 100 to 1000 mb, except for experiments denoted by an asterisk, where a layer from 200 to 1000 mb is used (see text).

ID	$\lvert\mathbf{u}' - \mathbf{c}\rvert$ (m s^{-1})	$\mathbf{u}'$ (°/m s^{-1})	at r =
D1	1.6	032/4.9	3°
D2	1.0	033/9.3	0°
J1*	1.8	302/2.8	3°
J2	1.0	005/2.4	3°
J3	0.6	014/3.4	3°
G1	0.6	316/5.7	3°
E2*	2.4	041/11.7	3°
A1	0.5	262/6.3	0°
E3	1.2	329/2.3	3°

TABLE 3. Magnitude of the vector difference, $|\mathbf{u}'_i - \mathbf{u}'|$ (m s^{-1}), between observed DLM wind ($\mathbf{u}'$) at the radius of better agreement (Table 2) and the corresponding DLM attributable to a piece of PV ($\mathbf{u}'_i$) confined to a cylinder of given radius (r) for each synoptic-flow experiment (ID) analyzed. As in Table 2, the DLM wind is calculated for the layer 100–1000 mb, except for experiments denoted by an asterisk, where a layer from 200 to 1000 mb is used (see text). A linear inversion was used except for the experiments denoted by two asterisks, where a nonlinear inversion was employed (see text).

r (km)	D1	D2	J1*	J2**	J3**	G1	E2*,**	A1	E3**
500	4.0	5.2	2.4	2.9	3.7	5.5	11.6	5.6	1.9
750	1.8	2.1	2.2	4.0	4.1	3.3	9.9	4.6	1.3
1000	2.0	2.6	2.9	4.5	4.1	0.5	8.5	4.1	1.5
1250	2.9	3.0	3.2	4.2	4.4	1.9	7.9	3.2	3.4
1500	3.0	3.3	2.8	4.1	5.4	2.0	8.2	2.5	5.3
2000	1.7	4.1	2.3	4.8	6.5	2.2	8.6	2.5	7.6
3000	—	—	—	—	—	—	—	—	5.0
4000	—	—	—	—	—	—	—	—	3.4

of Hurricane Emily of 1993 the radius of the cylinder could be extended to 4000 km. The same inversion technique described in the appendix of S96 was used, with the two constants (A and C) entering the coupled system of PV and balance equations [(A5) and (A6) of S96] chosen empirically to allow convergence. The default (Dirichlet) lateral boundary condition is that the geopotential anomaly is zero on the four edges of the domain. As found by Davis and Emanuel (1991) and S96, the inversion method does not converge unless the condition $q > 0$ is imposed. Two further limitations were found with the inversion. In two of the cases (marked by an asterisk in Tables 2 and 3) no combination of constants could be found where the system converged unless the top of the domain was lowered from 100 to 200 mb; then convergent solutions could be found. The linear piecewise inversion described in section 1 (following S96) was applied whenever possible. In four of the cases, however, no combination of constants could be found where the linear system converged. Although $q > 0$ ensures convergence of the *nonlinear* system there is no such guarantee for the linear one. When the linear system failed to converge the nonlinear terms were apparently not very small. In those cases (marked by two asterisks in Table 3) the nonlinear system was solved using the ad hoc partitioning of the nonlinear terms derived by Davis and Emanuel (1991), as described in section 3a of S96. It is possible that convergence of the piecewise inversion could have been achieved had another (unexamined) combination of constants been selected.

Table 3 presents the essential results of the piecewise inversions for each of the nine cases. The magnitude of the vector difference between the observed DLM wind at the radius of better agreement ($\mathbf{u}'$; Table 2) and the corresponding DLM attributable to pieces of PV confined to cylinders of a given radius ($\mathbf{u}'_i$) are presented. For Hurricane Gloria the smallest vector difference is $|\mathbf{u}'_i - \mathbf{u}'| = 0.5$ m s^{-1}, for a cylinder of radius 1000 km. The vector difference is 9% of the observed DLM. The vector representing the DLM attributable to PV within this cylinder is shown in the top panel of Fig. 1, together with the observed DLM. This result for Gloria is consistent with that for the benchmark analysis (S96), where the minimum vector difference (1.4 m s^{-1}) between the deduced DLM at the center of the hurricane and the storm's motion was found for a cylinder of the same radius. As in S96, the sensitivity of the results to the choice of homogeneous lateral boundary conditions has been evaluated. When the Dirichlet boundary conditions on the geopotential anomalies were replaced by Neumann conditions on the normal derivatives on opposite (either northern–southern or eastern–western) edges of the domain, the vector difference $|\mathbf{u}'_i - \mathbf{u}'|$ for a cylinder of radius 2000 km (the extent of the domain) changed by only ± 0.3 m s^{-1}. Thus, confirming the result of S96, the lateral boundaries do not significantly affect the results of the piecewise inversion for Gloria. A similar insensitivity was found for Hurricane Andrew (A1), the first of two experiments in Hurricane Debby (D1), and the first and third of three successive experiments in Hurricane Josephine (J1, J3) (other cases not being tested), giving confidence in the robustness of the results.

Four of the nine synoptic-flow cases have a relatively good match between the observed DLM wind near the center of the cyclone ($\mathbf{u}'$) and the DLM wind attributable to a cylinder of PV ($\mathbf{u}'_i$) with a given radius. For cases A1, G1, D1, and D2 the vector difference $|\mathbf{u}'_i - \mathbf{u}'|$ (Table 3) was $\leq 40\%$ of $|\mathbf{u}'|$ (Table 2) for a cylinder with some radius ≤ 1500 km.[3] Potential vorticity anomalies for these cases are shown in Fig. 1 for Hurricane Gloria, and Fig. 2 for Hurricane Andrew (A1), and two experiments in Hurricane Debby (D1, D2). As with the benchmark analyses the

[3] The use of the term "good" to describe a difference of 40% is of course, subjective.

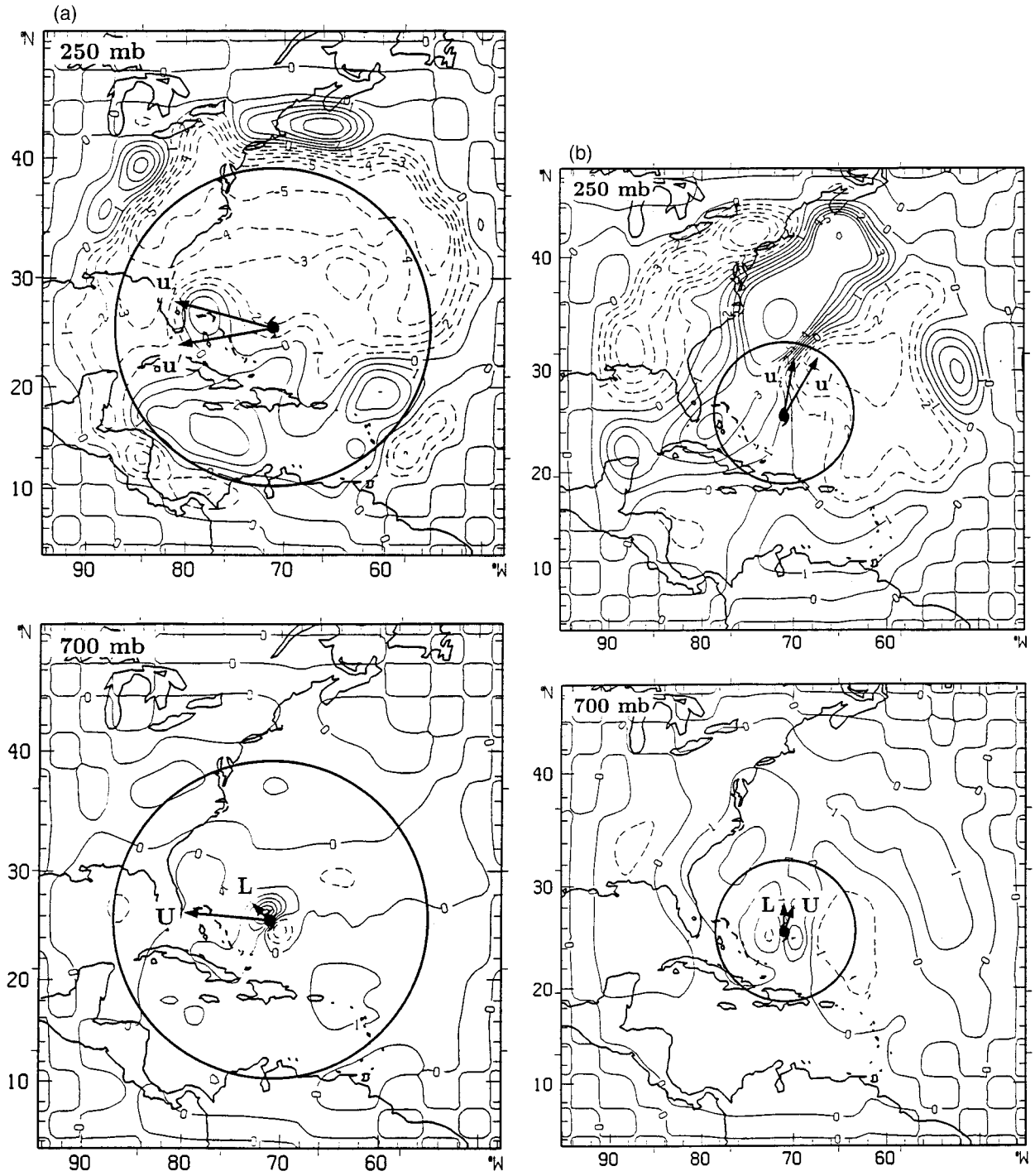

FIG. 2. Same as Fig. 1 but for synoptic-flow experiments (a) A1, (b) D1, and (c) D2 (see Table 1). Vectors in top panel for each experiment indicate observed DLM wind ($\mathbf{u}'$) at the radius of smaller difference from the respective storm's mean motion (Table 2) and the DLM wind ($\mathbf{u}_j'$) attributable to PV anomalies confined to a cylinder of radius 1500 km (A1), and 750 km (D1, D2), respectively [shown (slightly distorted)

cylinder with 1000-km radius surrounding Gloria that controls its steering flow, $\mathbf{u}'$ (to within 9%), incorporates the upper-level cold low to the southwest over Cuba (top panel of Fig. 1). Further decomposition of the PV anomaly into upper (400 mb and above) and lower levels (500 mb and below) indicates that the former anomaly explains 66% of the associated DLM wind anomaly, confirming the dominance of the upper-level features. Vectors representing the contributions from the upper- and lower-level PV anomalies

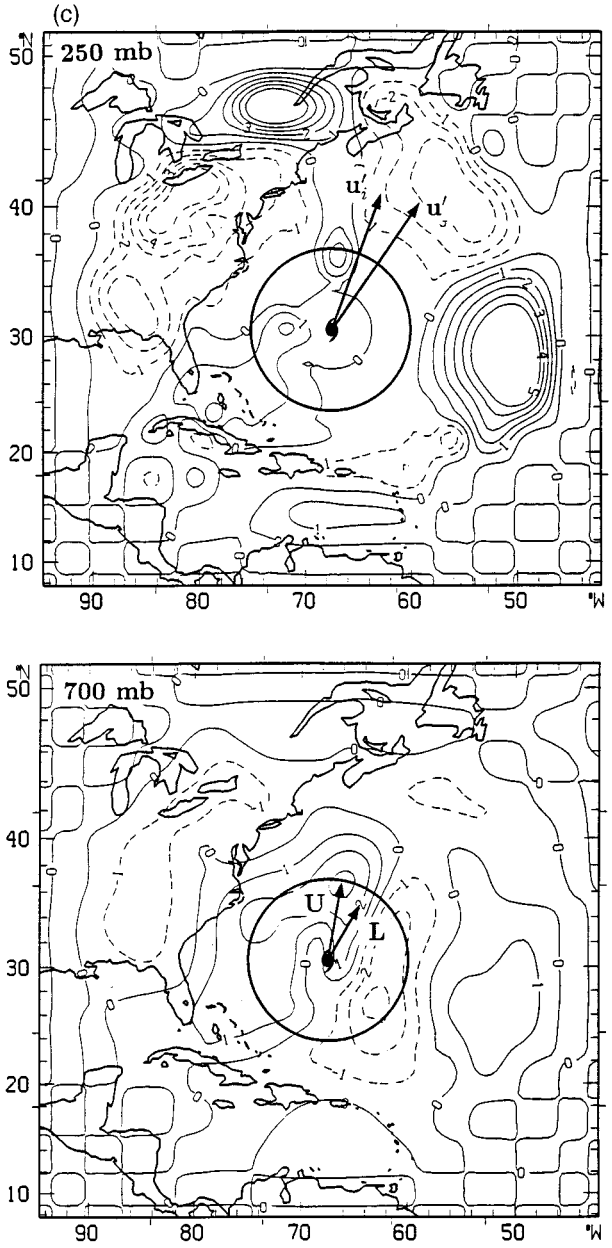

FIG. 2. *(Continued)* by circles in both panels]. Vectors in bottom panels indicate contributions to $\mathbf{u}_i'$ from upper-level (400 mb and above) PV anomalies (**U**) and lower-level (500 mb and below) PV anomalies (**L**).

are shown in the bottom panel of Fig. 1. The cylinder of 1500-km radius surrounding Andrew incorporates an upper-level north-to-south PV gradient (top panel of Fig. 2a) of a similar scale that determines its near-westward steering flow to within 40%. The upper-level PV anomaly explains 83% of the associated DLM wind anomaly (see bottom panel of Fig. 2a). Note that Andrew is the only case examined where the vector difference $|\mathbf{u}_i' - \mathbf{u}'|$ decreases outward monotonically for all cylinders with radii 500–2000 km.[4] The environment of Hurricane Debby during both experiments (Figs. 2a,b) has a nearly barotropic low at both upper and lower levels near 750 km from the hurricane's center. Correspondingly, PV confined to a cylinder of this radius explains the hurricane's northeastward steering flow to within 35% and 23% on the respective days (see top panels of Figs. 2a,b). Also, the upper- and lower-level PV anomalies explain nearly equal fractions of the associated DLM wind anomalies, with the upper level explaining 54% on both days (see bottom panels of Figs. 2b,c).

By contrast, five of the nine synoptic-flow cases do not have a good match between the observed DLM near the center of the cyclone and the DLM wind attributable to a cylinder of PV of any radius $\leq$2000 km. For the second experiment in Tropical Storm Emily of 1987 (E2), three successive experiments in Hurricane Josephine[5] (J1, J2, J3), and Hurricane Emily of 1993 (E3), the vector difference $|\mathbf{u}_i' - \mathbf{u}'|$ is greater than 50% of $|\mathbf{u}'|$ for all radii evaluated (Table 3). In these cases the minimum vector difference $|\mathbf{u}_i' - \mathbf{u}'|$ was 68% (E2), 78% (J1), 120% (J2), 109% (J3), and 54% (E3) of the respective DLM wind anomaly. As an example, PV anomalies for case J2 are shown in Fig. 3. Although the hurricane was moving nearly northward at the time of the analysis, PV features nearby appear to move the cyclone to the west. This tendency was confirmed in the PV inversions and resulted in the substantial vector differences for this case. Due to the larger analysis domain in the case of Hurricane Emily of 1993, cylinders of radii up to 4000 km could be evaluated. Although the vector difference $|\mathbf{u}_i' - \mathbf{u}'|$ decreased monotonically outward from 2000 km, the difference for a 4000-km cylinder (3.4 m s^{-1}) was still $\gg$ the observed DLM wind speed (2.3 m s^{-1}). This result implies that PV anomalies on a very large scale ($\gg$4000 km) are required to explain the steering flow that advected this hurricane.

3. Discussion and conclusions

The results from the nine synoptic-flow cases can be loosely placed into two categories describing the spatial scale of the PV anomalies that influence the cyclones' motion. Cases with ''local'' control have a ''good'' match (to within ~40%) between the observed DLM wind near the center of the cyclone and the DLM attributable to a cylinder of PV centered on the cyclone with a given radius $\leq$1500 km. Although PV anomalies outside of this region make a contribution to the DLM steering flow, the short-term changes in this flow are

[4] For a cylinder of sufficiently large radius ($\gg$2000 km) the inversion in all cases must reproduce the complete steering flow, giving $|\mathbf{u}_i' - \mathbf{u}'| = 0$. See also footnote 6.

[5] During the first experiment, Josephine had not yet achieved hurricane strength and was classified as a tropical storm.

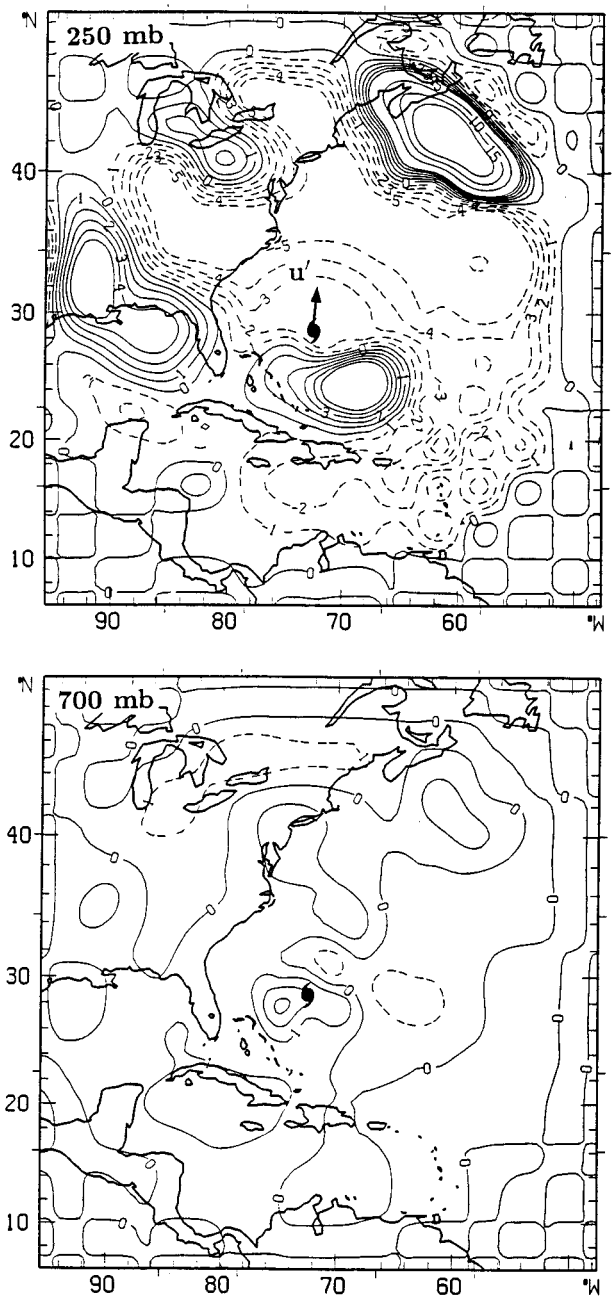

FIG. 3. Same as Fig. 1 but for the second of three successive synoptic-flow experiments in Hurricane Josephine (J2). Solid vector in top panel indicates observed DLM wind at radius r = 3°.

determined primarily by features within. Four of the cases, both experiments in Hurricane Debby (D1, D2), Hurricane Gloria (G1), and Hurricane Andrew (A1), fell into this category. When the PV anomalies controlling the cyclones' motion were decomposed into upper (400 mb and above) and lower levels (500 mb and below), it was found that two of the cases (G1 and A1) were dominated by upper-level features and two other cases (D1 and D2) had nearly equal contributions from each level. The control of the upper-level cold low over Cuba in the case of Gloria simply confirms the results of S96 for the benchmark analyses. The dominance of upper-level steering in the case of Andrew supplements the results of Wu and Emanuel (1995b), who found that PV anomalies 300 mb and below contributed more than anomalies 250 mb and above to steering the hurricane. Besides the different definitions of ''upper'' and ''lower'' layer, the inclusion of a substantial climatological mean component in Wu and Emanuel's (1995b) analysis (see their Fig. 10) precludes a direct comparison with their results. In the case of Hurricane Debby, control of the cyclone's motion by a nearly barotropic low to its north confirms both synoptic intuition and results of numerical track forecasts (Burpee et al. 1984; Burpee et al. 1996).

Synoptic-flow cases with ''large-scale'' control, by contrast, have no cylinder with radius $\leq$2000 km with a good match between the DLM wind attributable to PV confined within the cylinder and the observed DLM wind. Five of the cases, Hurricane Emily of 1987 (E2), Hurricane Emily of 1993 (E3), and all three experiments in Hurricane Josephine (J1, J2, and J3) fell into this category. As with the second successive experiment in Josephine (J2), shown in Fig. 3, each of these cases evidenced nearby PV anomalies that moved the cyclone in a direction contrary to the DLM steering flow near its center. For these cases, by implication, the short-term changes in the steering flow are determined primarily by PV anomalies outside of 2000 km from the center.[6] It is interesting that it is just for these cases that the linear piecewise inversion failed to converge for the full depth of the domain. It is not clear, however, to what extent this result is coincidental. In the case of Hurricane Josephine, Franklin (1990) found that track forecasts with a barotropic numerical model were quite problematic. The results of the present analyses indicate that accurate DLM winds over a distance $\gg$2000 km surrounding Josephine are required to properly represent short-term changes in the environmental flow field that steered the hurricane.

Simple inspection of the PV anomaly fields gives no obvious indication of which cases have local control and which have large-scale control. Only the piecewise PV inversion can clearly distinguish between the two situations. It is significant that for both hurricanes for which experiments on successive days were analyzed, the characterization of local versus large-scale control was invariant: the motion of Hurricane Debby was con-

[6] In the context of a PV inversion in a finite domain, these ''nonlocal'' PV anomalies would include the contribution to the wind from nonhomogeneous lateral boundary conditions. By construction, an inversion using PV anomalies over the full domain and nonhomogeneous boundary conditions must reproduce the complete steering flow, giving a perfect match between the deduced and observed DLM wind.

trolled by local PV anomalies on both days; the motion of Hurricane Josephine was controlled by large-scale PV anomalies on all three days. Thus, the methodology presented here has potential as an aid in guiding the deployment of operational and research aircraft that make in situ wind measurements of the hurricane's environment. Once it was established, from measurements centered on 0000 UTC 15 September 1982, that Hurricane Debby was steered by winds determined primarily by PV features within 1000 km of its center, observations on the next day that were designed to improve short-term track forecasts would naturally be concentrated in this near-hurricane environment. For Josephine, measurements centered on 0000 UTC 10 October 1984 established that the hurricane was steered by winds determined primarily by PV anomalies outside of 2000 km from its center. Observations on successive days would naturally be spread over a wider domain.

Track forecast verifications for a barotropic numerical model (DeMaria et al. 1992) initialized with and without ODW observations provide a confirmation of the present results. Those cases with local control had a much greater average reduction in track forecast error due to the ODW observations than did the cases with large-scale control for all forecast periods 12–72 h, averaging 39% reduction in the former cases versus 12% in the latter. The obvious interpretation is that ODW observations, which sample PV features near a tropical cyclone, are more effective in improving track forecasts for cases of local control, where short-term changes in the steering flow are determined primarily by PV features also near the cyclone.

Acknowledgments. This research was supported in part by the Office of Naval Research Grant N00014-93-1-0456 to the Department of Atmospheric Science, Colorado State University. The first author would like to thank Dr. Dominique Möller for many helpful discussions during the course of this work.

REFERENCES

Burpee, R. W., D. G. Marks, and R. T. Merrill, 1984: An assessment of dropwindsonde data in track forecasts of Hurricane Debby (1982). *Bull. Amer. Meteor. Soc.,* **65,** 1050–1058.

——, J. L. Franklin, S. J. Lord, R. E. Tuleya, and S. D. Aberson, 1996: The impact of Omega dropwindsondes on operational hurricane track forecast models. *Bull. Amer. Meteor. Soc.,* **77,** 925–933.

Davis, C. A., 1992: Piecewise potential vorticity inversion. *J. Atmos. Sci.,* **49,** 1397–1411.

——, and K. A. Emanuel, 1991: Potential vorticity diagnostics of cyclogenesis. *Mon. Wea. Rev.,* **119,** 1925–1953.

DeMaria, M., S. D. Aberson, K. V. Ooyama, and S. J. Lord, 1992: A nested spectral model for hurricane track forecasting. *Mon. Wea. Rev.,* **120,** 1628–1643.

Franklin, J. L., 1990: Dropwindsonde observations of the environmental flow of Hurricane Josephine (1984): Relationships to vortex motion. *Mon. Wea. Rev.,* **118,** 2732–2744.

——, S. J. Lord, S. E. Feuer, and F. D. Marks Jr., 1993: The kinematic structure of Hurricane Gloria (1985) determined from nested analyses of dropwindsonde and Doppler radar data. *Mon. Wea. Rev.,* **121,** 2433–2451.

——, S. E. Feuer, J. Kaplan, and S. D. Aberson, 1996: Tropical cyclone motion and surrounding flow relationships: Searching for beta gyres in Omega dropwindsonde datasets. *Mon. Wea. Rev.,* **124,** 64–84.

Möller, J. D., and S. C. Jones, 1998: Potential vorticity inversion for tropical cyclones using the asymmetric balance theory. *J. Atmos. Sci.,* **55,** 259–282.

Ooyama, K. V., 1987: Scale controlled objective analysis. *Mon. Wea. Rev.,* **115,** 2479–2506.

Shapiro, L. J., 1996: The motion of Hurricane Gloria: A potential vorticity diagnosis. *Mon. Wea. Rev.,* **124,** 2497–2508.

——, and M. T. Montgomery, 1993: A three-dimensional balance theory for rapidly rotating vortices. *J. Atmos. Sci.,* **50,** 3322–3335.

——, and J. L. Franklin, 1995: Potential vorticity in Hurricane Gloria. *Mon. Wea. Rev.,* **123,** 1465–1475.

Wu, C.-C., and K. A. Emanuel, 1995a: Potential vorticity diagnosis of hurricane movement. Part I: A case study of Hurricane Bob (1991). *Mon. Wea. Rev.,* **123,** 69–92.

——, and ——, 1995b: Potential vorticity diagnosis of hurricane movement. Part II: Tropical Storm Ana (1991) and Hurricane Andrew (1992). *Mon. Wea. Rev.,* **123,** 93–109.

——, and Y. Kurihara, 1996: A numerical study of the feedback mechanisms of hurricane-environment interaction on hurricane movement from the potential vorticity perspective. *J. Atmos. Sci.,* **53,** 2264–2282.